Magnetic phase transitions in a light wave

A. F. Kabychenkov

Institute of Radio Engineering and Electronics, Academy of Sciences of the USSR
(Submitted 19 October 1990; resubmitted 29 May 1991)
Zh. Eksp. Teor. Fiz. **100**, 1219–1237 (October 1991)

The effect of an intense light wave on the magnetization of a transparent cubic ferromagnet is studied. Phase diagrams are constructed for a material in the field of a light wave near the Curie point and in the vicinity of an orientational phase transition. The change in the magnetization can occur by a first- or second-order phase transition, depending on the values of the homogeneous-exchange constant and the crystallographic-anisotropy constant. The critical and bicritical points are calculated. The effect of light on domain walls and on the domain structure is analyzed. The changes in the width of domain walls, in the period of the domain structure, and in the orientation of this structure are calculated. The effect of pinning of the magnetic moment at the surface on the light-induced phase transition is analyzed. A phase diagram is constructed for a ferromagnetic plate; inhomogeneous states are taken into account.

A light wave interacts with a magnetic subsystem of a magnetic material through the electric component of the wave field, by virtue of the magnetization dependence of the dielectric constant.[1)] The interaction changes the characteristics of both the light and the magnetic subsystem. If the components of the magnetic energy (the inhomogeneous exchange energy, the anisotropy energy, and the magnetic-dipole energy) are large in comparison with the interaction energy, the changes are primarily in the light. Examples are the classic magnetooptic effects of circular and linear birefringence.

If these energies satisfy the opposite inequalities, the primary changes are in the magnitude and direction of the magnetic moments of the sublattices. These changes can be thought of as inverse magnetooptic effects, i.e., optomagnetic effects. Optomagnetic effects stem from the constant effective magnetic fields which arise from the nonlinear interaction of the light wave with the magnetic subsystem. Since the magnetooptic constants are small, and the optomagnetic effects are quadratic in the electric field of the wave, the light has only a weak effect on the magnetization, even if it is relatively intense. Nevertheless, near phase transitions, where the susceptibility is anomalously large, even weak effects can cause substantial changes in the magnetic subsystem, including light-induced phase transitions.

The magnetization of a transparent nonmagnetic medium by an alternating electric field was studied in Ref. 1. The inverse Faraday effect in paramagnets was studied in Ref. 2. Relations given in Ref. 2 were used in Ref. 3 to estimate the light-induced magnetization of magnetic semiconductors. This effect was studied in magnetic insulators in detail in Ref. 4. The inverse Cotton–Mouton effect in ferromagnets was studied theoretically in Refs. 5 and 6. It has been observed experimentally in iron garnet films containing bismuth.[7]

In the present paper we are interested in magnetic spontaneous and orientational phase transitions caused by a light wave in a transparent cubic ferromagnetic crystal. We examine the effect of light on domain walls and the domain structure. We studied the effect of pinning of the magnetic moment on the light-stimulated phase transition. We should point out that optomagnetic effects differ from photomagnetic effects.[8] The former are unrelated to the absorption of the light and are seen most obviously in transparent crystals. The light wave simply produces effective magnetic fields. In the latter case, the light, as it is absorbed, excites electrons into the conduction band or into localized energy levels. As a result the electron density becomes redistributed; this redistribution in turn causes changes in the properties of the magnetic subsystem: the homogeneous- and inhomogeneous-exchange constants, the anisotropy, the energy of the pinning of the magnetic moment at defects, and other parameters.

BASIC EQUATIONS

The energy density of the magnetic subsystem of a transparent ferromagnet in the field of a monochromatic light wave can be written

$$w=f(\mathbf{M}^2)+\frac{1}{2}a_{ij}\frac{\partial \mathbf{M}}{\partial x_i}\frac{\partial \mathbf{M}}{\partial x_j}+w_a(M_i^2)-\mathbf{M}\left(\mathbf{H}-\frac{1}{2}\mathbf{H}_p\right)$$
$$-\frac{1}{2}\chi_{ij}H_iH_j-\frac{1}{16\pi}\varepsilon_{ij}E_i^*E_j. \qquad (1)$$

The terms in (1) determine the energy of the homogeneous and inhomogeneous exchange, the anisotropy energy, the magnetic-dipole energy, and the average energy of the magnetic material in the field of the light. Here $\mathbf{M}$ is the (vector) magnetic moment, a_{ik} are the homogeneous-exchange constants, $\mathbf{H}=\mathbf{H}_0+\mathbf{H}_d$ is the internal magnetic field, $\mathbf{H}_0$ is the external magnetic field, $\mathbf{H}_d$ is the demagnetizing field, χ_{ij} is the susceptibility of the paraprocess, E_i are components of the complex amplitude of the electric field of the wave,

$$\vec{\mathscr{E}}=[\mathbf{E}\exp(i\omega t)+\mathbf{E}^*\exp(-i\omega t)]/2,$$

and ω is the frequency of the light. The dielectric tensor is written in the form

$$\varepsilon_{ij}=\varepsilon_{ij}^{(0)}+ie_{ijk}(\alpha_{kn}M_n+\alpha_{kn}'H_n)+\beta_{ijkn}M_kM_n$$
$$+\beta'_{ijkn}M_kH_n+\beta''_{ijkn}H_kH_n, \qquad (2)$$

where $\varepsilon_{ij}^{(0)}$ is the dielectric tensor of the paramagnetic phase in the absence of $\mathbf{H}$, e_{ijk} is the Levi–Civita tensor, and $\hat{\alpha}$ and $\hat{\beta}$ are the circular and linear birefringence tensors, whose values are taken at the frequency of the wave. The terms

 0038-5646/91/100672-11$03.00

which contain H_n determine the anisotropy $\hat{\varepsilon}$ induced by the external field while those containing M_n determine the intrinsic anisotropy, which is a consequence of the homogeneous-exchange field $H^{(e)}$. In the ferromagnetic phase far from the Curie point T_C the condition $H^{(e)} \gg H$ usually holds. As T_C is approached, the quantity $H^{(e)}$ decreases, and the effect of H becomes noticeable. Near T_C the external field stimulates the exchange interaction, thereby increasing $H^{(e)}$. The effect of the field H on the direct and inverse magnetooptic effects was studied in Refs. 9 and 10. In the paramagnetic phase far from T_C, the terms linear and quadratic in H become the leading terms. The linear term gives us the magnetization change,

$$\Delta M_n = -[\partial w(E_i)/\partial H_n]|_0 = ie_{ijk}\alpha_{kn}' E_i^* E_j/16\pi,$$

and the quadratic term gives us the change in the paramagnetic susceptibility,

$$\Delta\chi_{ij} = -[\partial^2 w(E_i)/\partial H_i\,\partial H_j]|_0 = \beta_{ijkl}'' E_k^* E_l/16\pi.$$

In the absence of an external magnetic field, the light does not affect the state of a paramagnet.

The amplitude $\mathbf{E}$ satisfies the equations

$$\frac{\partial^2 E_i}{\partial x_k\,\partial x_k} - \frac{\partial^2 E_k}{\partial x_i\,\partial x_k} + \frac{\omega^2}{c^2}\varepsilon_{ij}E_j = 0, \quad \frac{\partial(\varepsilon_{ij}E_j)}{\partial x_i} = 0, \qquad (3)$$

where c is the velocity of light.

The energy density of a cubic magnetic material in the vicinity of the ferromagnetic phase can be written as follows, where we are using (1) and (2):

$$\begin{aligned} w = {} & f(\mathbf{M}^2) + \frac{a}{2}\left(\frac{\partial \mathbf{M}}{\partial x_k}\right)^2 + K_{12}(M_x^2M_y^2 + M_x^2M_z^2 + M_y^2M_z^2) \\ & + K_{112}[M_x^4(M_y^2+M_z^2) + M_y^4(M_x^2+M_z^2) \\ & + M_z^4(M_x^2+M_y^2)] + K_{123}M_x^2M_y^2M_z^2 \\ & - \frac{1}{16\pi}[\beta_2\mathbf{M}^2|\mathbf{E}|^2 + \bar{\beta}(M_x^2|E_x|^2 + M_y^2|E_y|^2 + M_z^2|E_z|^2) \\ & + \beta_3(\mathbf{ME})(\mathbf{ME}^*)] - \mathbf{M}\left[\left(1 + \frac{\beta_2'}{16\pi}|\mathbf{E}|^2\right)\mathbf{H} + \mathbf{G}\right] \\ & - \frac{\bar{\beta}'}{16\pi}(M_xH_x|E_x|^2 + M_yH_y|E_y|^2 + M_zH_z|E_z|^2) + \frac{1}{2}\mathbf{MH}_p. \end{aligned} \qquad (4)$$

Here $a_{ik} = a\delta_{ik}$; K_{12}, K_{112}, K_{123} are the crystallographic-anisotropy constants; and

$$\beta_1^{(\prime)} = \beta_{1111}^{(\prime)} = \beta_{2222}^{(\prime)} = \beta_{3333}^{(\prime)}, \quad \beta_2^{(\prime)} = \beta_{1122}^{(\prime)} = \beta_{1133}^{(\prime)} = \beta_{2233}^{(\prime)},$$

$$\beta_3^{(\prime)} = \beta_{1212}^{(\prime)} = \beta_{1313}^{(\prime)} = \beta_{2323}^{(\prime)}, \quad \bar{\beta}^{(\prime)} = \beta_1^{(\prime)} - \beta_2^{(\prime)} - \beta_3^{(\prime)},$$

$$\mathbf{G} = i\alpha[\mathbf{E}^*\mathbf{E}]/16\pi, \quad \alpha = \alpha_{11} = \alpha_{22} = \alpha_{33}.$$

It can be seen from expression (4) that the light wave creates an additional anisotropy and a magnetic field $\mathbf{G}$, and in a field $\mathbf{H}$ it also creates an additional magnetization. The symmetry of the light-induced anisotropy depends on the polarization and propagation direction of the wave. The quantity $\mathbf{G}$ is determined by the ellipticity of the polarization. For a linearly polarized wave we would have $\mathbf{G} = 0$. The components of the vector $\mathbf{M}$ change by the following amount in the field of the light by virtue of the effect of $\mathbf{H}$:

$$\Delta M_i = (\beta_2'|\mathbf{E}|^2 + \bar{\beta}'|E_i|^2)/16\pi.$$

This change consists of an isotropic part and an anisotropic part. Near T_C the inhomogeneous-exchange energy can be written in the following form, within the range of applicability of the self-consistent-field theory:

$$f = f_0 + {}^1/_2 A\mathbf{M}^2 + {}^1/_4 B\mathbf{M}^4. \qquad (5)$$

It follows from (4) and (5) that the wave also creates an additional exchange field. If we set $A = A'(T - T_C)$, the isotropic effect of the light reduces to a shift of T_C by an amount $\Delta T_C = \beta_2|\mathbf{E}|^2/8\pi A'$. The direction of this shift in T_C depends on the sign of β_2, since we have $A' > 0$.

In a plane wave, the longitudinal component E_x is related to the transverse components E_y and E_z by the following relation, as can be seen from (3):

$$E_x = -(\varepsilon_{xy}E_y + \varepsilon_{xz}E_z)/\varepsilon_{xx}.$$

Since the off-diagonal components of the tensor $\hat{\varepsilon}$ are determined by small magnetooptic constants, the component E_x can be ignored. In this case the field $\mathbf{G}$ will be directed along the light beam.

SPONTANEOUS PHASE TRANSITIONS

The effective magnetic fields produced by the light wave may alter the state of the magnetic material. We first consider spontaneous phase transitions which occur between homogeneous states in the field of a wave which is polarized linearly along the z axis and which is propagating along the x axis, in a direction parallel to an edge of the cubic cell. Near T_C we can restrict the discussion to the first anisotropy constant. In the absence of a magnetic field, expression (4) then becomes

$$w = {}^1/_2 A_1\mathbf{M}^2 + {}^1/_4 B\mathbf{M}^4 + K_{12}(M_x^2M_y^2 + M_x^2M_z^2 + M_y^2M_z^2) - U_1M_z^2, \qquad (6)$$

where $A_1 = A - 2\beta_2 U_0$ is the homogeneous-exchange constant as renormalized by the light field, $U_0 = |E_z|^2/16\pi$ is the energy density of the light field in vacuum, and $U_1 = (\beta_1 - \beta_2)U_0$ is the constant of the light-induced anisotropy. In the case at hand, the light shifts T_C and creates uniaxial anisotropy in addition to the cubic anisotropy. The axis of this new anisotropy runs parallel to an edge of the cube. Under the condition $\beta_1 > \beta_2$, there is an easy-axis anisotropy, while under the condition $\beta_1 < \beta_2$ there is an easy-plane anisotropy. Minimizing (6), we find the system of equations

$$\begin{aligned} \mu_{x,y}M_{x,y} &= (A_1 + CM^2 - 2K_{12}M_{x,y}^2)M_{x,y} = 0, \\ \mu_zM_z &= (A_1 + CM^2 - 2K_{12}M_z^2 - 2U_1)M_z = 0, \end{aligned} \qquad (7)$$

where $C = B + 2K_{12}$. From (7) we find the stationary states

1) $\mathbf{M}^{(1)} = 0$; 2) $(M_x^2)^{(2)} = -A_1/B$, $M_y^{(2)} = M_z^{(2)} = 0$;
3) $(M_y^2)^{(3)} = (M_x^2)^{(2)}$, $M_x^{(3)} = M_z^{(3)} = 0$;
4) $(M_z^2)^{(4)} = -(A_1 - 2U_1)/B$, $M_x^{(4)} = M_y^{(4)} = 0$;
5) $(M_x^2)^{(5)} = (M_y^2)^{(5)} = -A_1/2(B + K_{12})$, $M_z^{(5)} = 0$;
6) $(M_x^2)^{(6)} = \dfrac{Q+P}{2}$, $(M_z^2)^{(6)} = \dfrac{Q-P}{2}$, $M_y^{(6)} = 0$,

$$Q = \frac{U_1 - A_1}{B + K_{12}}, \quad P = \frac{U_1}{K_{12}}; \qquad (8)$$

7) $(M_y^2)^{(7)}=(M_x^2)^{(6)}$, $(M_z^2)^{(7)}=(M_z^2)^{(6)}$, $(M_x^2)^{(7)}=0$;

8) $(M_x^2)^{(8)}=(M_y^2)^{(8)}=\frac{R+P}{3}$, $(M_z^2)^{(8)}=\frac{R-2P}{3}$,

$$R=\frac{2U_1-3A_1}{3B+4K_{12}}.$$

Phase 1 is paramagnetic, while the other phases are ferromagnetic. In states 2, 3, and 4, the vector **M** is oriented along the [001] crystallographic direction (an edge of the cube). In state 5, the vector **M** is directed along the [110] axis (a diagonal of the base of the cube). In states 6, 7, and 8, the magnetization vector lies in, respectively, the (100) plane, the (010) plane (lateral faces of the cube), and the (110) plane (the plane which passes through the diagonal of the base and the edge of the cube which is normal to it).

The states determined by (8) are locally stable if all the principal minors of the determinant $|\partial^2 w/\partial M_i \partial M_j|$ are positive:

$$\mu_x+2BM_x^2>0,\quad d=(\mu_x+2BM_x^2)(\mu_y+2BM_y^2)-4C^2M_x^2M_y^2>0,$$
$$d(\mu_z+2BM_z^2)+4C^2M_z^2(8K_{12}M_x^2M_y^2-\mu_xM_y^2-\mu_yM_x^2)>0. \tag{9}$$

Substituting (8) into (9), we can determine the stability of the phases. The paramagnetic phase is stable in the region $A_1\geqslant\max(0,2U_1)$. The equality sign here corresponds to the line on which stability is lost. A necessary condition for the stability of the ferromagnetic phases is $B>0$. Phases 2 and 3 are stable under the condition $K_{12}>0$ in the region $A_1\leqslant\min(0,-bU_1)$, where $b=B/K_{12}$. Phase 4 is stable in the region $A_1\leqslant\min[2U_1,(2+b)U_1]$ if we have $K_{12}>0$ and in the interval $(2+b)U_1\leqslant A_1\leqslant 0$ if we have $-B<K_{12}<0$, $U_1<0$. The stability regions of phases 2, 3, and 4 overlap. Phase 5 is stable in the region $-2(1+b)U_1\leqslant A_1\leqslant 0$ if we have $-B<K_{12}<0$, $U_1<0$. Phases 6 and 7 are unstable. The vector **M** may pass through these states in the case of a nonuniform distribution of the magnetization. Phase 8 is stable in the region $A_1\leqslant\min[(2+b)U_1,\ -2(1+b)U_1]$ if $-3B/4<K_{12}<0$.

A stable phase with the minimum energy corresponds to the ground state. Substituting (8) into (6), we find the energies of the phases to be

$$w^{(1)}=0,\quad w^{(2)}=w^{(3)}=-\frac{A_1^2}{4B},\quad w^{(4)}=-\frac{(A_1-2U_1)^2}{4B},$$
$$w^{(5)}=-\frac{A_1^2}{4(B+K_{12})},\quad w^{(8)}=-\frac{1}{3}\left[\frac{1}{4}(3B+4K_{12})R^2+U_1P\right]. \tag{10}$$

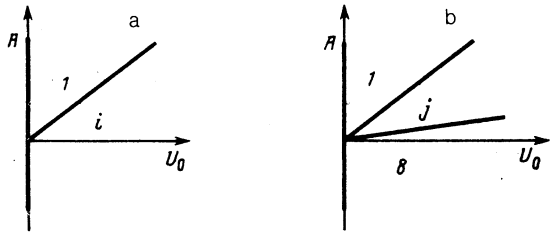

FIG. 1. Phase diagrams of a cubic ferromagnet in the vicinity of a spontaneous phase transition in the field of a linearly polarized wave. a—$K_{12}>0$, $i=2,3$ for $\beta_1<\beta_2$ and $i=4$ for $\beta_1>\beta_2$; b—$K_{12}<0$, $j=5$ for $\beta_1<\beta_2$ and $j=4$ for $\beta_1>\beta_2$.

Phases 2 and 3 have identical energies. For phases 2, 3, and 4, we have $w^{(2)}\gtrless w^{(4)}$ under the conditions $U_1\gtrless 0$, respectively, in the stability region.

We can determine the phase boundaries by equating the energies (10) of the phases with overlapping stability regions. The boundaries between the paramagnetic and ferromagnetic phases 2, 3, 4, and 5 correspond to the relation $A_1=2\max(0,U_1)$, The boundaries between ferromagnetic phases 4 and 8, 5 and 8 are determined by the relations $A_1=(2+b)U_1$, $A_1=-2(1+b)U_1$. These phase boundaries coincide with lines of loss of stability. When these boundaries are crossed, the magnetization changes continuously, according to (8). The change in state occurs through a second-order phase transition (PT-II).

As a result, two phases exist at $K_{12}>0$: a paramagnetic phase and one of the ferromagnetic phases 2, 3, 4. The crystallographic anisotropy gives rise to three special axes, along the edges of the cube. The light-induced anisotropy partially lifts the degeneracy. If this is an easy-axis anisotropy ($U_1>0$), the magnetization is directed along the polarization axis, parallel to the [001] edge. If the induced anisotropy is instead an easy-plane anisotropy ($U_1<0$), the vector **M** lies in the basal plane, along the [100] or [010] axis. Under the condition $K_{12}<0$, three phases exist: the paramagnetic phase and two ferromagnetic phases, 8 and either 4 or 5, under the conditions $U_1\gtrless 0$, respectively. In this case the crystallographic anisotropy gives rise to special axes along the body diagonals. The light-induced anisotropy deflects **M** toward the [001] axis in the (110) plane if this is an easy-axis anisotropy; alternatively, it deflects it toward the [110] axis if this is an easy-plane anisotropy.

Figure 1a, b, shows a state diagram in terms of the independent variables A, U_0. The behavior of the magnetization with increasing field energy depends on the initial state of the magnetic material and on the direction in which T_C shifts. For $A\beta_M<0$ [$\beta_M=\max(\beta_1,\beta_2)$], the paramagnetic and ferromagnetic states persist. For $A,\beta_M>0$ the magnetic material goes from a paramagnetic state to a ferromagnetic state. For $A,\beta_M<0$, on the contrary, it goes from a ferromagnetic state to a paramagnetic state. Under the condition $K_{12}<0$, phase transition can occur between the various ferromagnetic phases. In the case $\beta_1<\beta_2$, the magnetic material goes from state 4 into state 8 or in the opposite direction, from state 8 to 4, under the conditions A, $2\beta_1+b(\beta_1-\beta_2)\gtrless 0$, respectively. In the case $\beta_1<\beta_2$, phase 5 is replaced by phase 8, or vice versa, under the conditions A, $\beta_2-(1+b)(\beta_1-\beta_2)\gtrless 0$, respectively.

In specific situations, the change in the magnetization with increasing U_0 occurs in the following way. Let us assume that in the absence of the light the magnetic material is in the paramagnetic state ($A>0$). In the case $\beta_1>\beta_2$ or $\beta_1>0$, the magnetization **M** is then zero as long as the condition $U_0\leqslant A/2\beta_1$ holds. A component M_z then arises. If we have $K_{12}<0$, then in the region

$$U_0>A/[2\beta_1+b(\beta_1-\beta_2)]>0$$

the components M_x and M_y also begin to grow. Under the condition $\beta_1<0$, the state does not depend on U_0. In the case $\beta_1<\beta_2$ with $\beta_2>0$, the component M_x or M_y increases in the region $U_0>A/2\beta_2$ if the condition $K_{12}>0$ holds; alter-

natively, the two components M_x and M_y increase simultaneously if $K_{12}<0$. In the latter case, with

$$U_0>A/2[\beta_2-(1+b)(\beta_1-\beta_3)]>0$$

a component M_z also appears. If $\beta_2<0$ holds, the light does not alter the state of the magnetic material. The initial ferromagnetic state changes in the opposite order as a function of U_0.

Let us examine the behavior of the magnetization in a circularly polarized wave which is propagating parallel to the direction of the magnetic field, along the x axis. Since the field **H** lifts the degeneracy with respect to the direction of **M**, a slight anisotropy can be ignored near T_C. For a left-hand circular polarization ($E_z=-iE_y$), expression (4) then reduces to the following expression, where we are using (5):

$$w={}^1/_2A_2\mathbf{M}^2+{}^1/_4B\mathbf{M}^4+U_1M_x^2-M_xH_\Sigma, \tag{11}$$

where $A_2=A-2(\beta_1+\beta_2)U_0$, $H_\Sigma=H+\gamma U_0$, $\gamma=2\alpha+(\beta_1'+\beta_2'-\beta_3')H$. In this case, as in the preceding case, the light shifts T_C and gives rise to uniaxial anisotropy. In the present case, on the other hand, the anisotropy is parallel to the light propagation direction, and the anisotropy constant has the opposite sign: It is an easy-axis or easy-plane anisotropy under the conditions $\beta_1\lesseqgtr\beta_2$. In addition, the light gives rise to an effective magnetic field along the light-propagation direction or in the opposite direction, under the conditions $\alpha\gtreqless0$. It also renormalizes the magnetic-dipole energy.

Minimizing (11) under the condition $H_\Sigma\neq0$, we find $M_y^{(0)}=M_z^{(0)}=0$, and we find that $M_x^{(0)}$ satisfies the equation

$$[A_3+B(M_x^{(0)})^2]M_x^{(0)}=H_\Sigma, \tag{12}$$

where $A_3=A-4\beta_2U_0$. Since we have $M_x^{(0)}\neq0$ according to (12), a spontaneous phase transition does not occur in this case. Nevertheless, the structural features in the changes in M persist, and in the limit $H_\Sigma\to0$ they are strengthened. In the weak-field region, $|h|=|H_\Sigma|/H_C\ll1$, where we have $H_C=|A_3|^{3/2}B^{-1/2}$, we have

$$M_x^{(0)}=A_3^{-1}H_\Sigma(1-h^2) \tag{13}$$

in the "paramagnetic" phase ($A_3>0$) and

$$M_x^{(0)}=(-A_3)^{-1}H_C({}^1/_2h\pm1) \tag{14}$$

in the "ferromagnetic" phase ($A_3<0$). The value of $M_x^{(0)}$ which is greatest in magnitude in (14) (the $\pm$ signs correspond to the conditions $H_\Sigma\gtreqless0$) corresponds to the ground state.[2] In the strong-field region, $|h|\gg1$, we have

$$M_x^{(0)}=\left(\frac{H_\Sigma}{B}\right)^{1/3}\left(1+\frac{1}{3h^{2/3}}\right). \tag{15}$$

If $A\beta_2<0$, the state of the magnetic material does not change as U_0 varies. In the case $A\lesseqgtr0$, the initial ferromagnetic (or paramagnetic) state goes into a paramagnetic (or, respectively, ferromagnetic) state under the conditions $\beta_2\lesseqgtr0$. Working from (13)–(15), we can introduce the susceptibility

$$\chi_c=\frac{\partial M_x^{(0)}}{\partial U_0}\approx\begin{cases}\dfrac{\gamma+4\beta_2H_\Sigma A_3^{-1}}{A_3}\left[1-h^2\left(3+\dfrac{1}{1+\gamma A_3(4\beta_2H_\Sigma)^{-1}}\right)\right], & A_3>0,\quad |h|\ll1\\ \dfrac{\gamma\mp4\beta_2H_CA_3^{-1}}{-2A_3}\left[1-\dfrac{h}{2}\left(\dfrac{1}{\gamma A_3(4\beta_2H_C)^{-1}\mp1}\pm3\right)\right], & A_3<0,\quad |h|\ll1.\\ \dfrac{\gamma+4\beta_2(H_\Sigma/B)^{1/3}}{3B^{1/3}H_\Sigma^{2/3}}\left[1-\dfrac{1}{3h^{2/3}}\left(2+\operatorname{sign}A_3-\dfrac{1}{\gamma B^{1/3}(4\beta_2H_\Sigma^{1/3})^{-1}+1}\right)\right], & |h|\gg1.\end{cases} \tag{16}$$

In general, the functional dependence (16) is quite complicated, since U_0 changes the two parameters A_3 and H_Σ simultaneously. The function χ_c differs substantially from the ordinary $\chi(T,H)$. In the weak-field region in the paramagnetic state we have

$$\chi_c\approx(A\gamma+4\beta_2H)/A_3^2\propto A_3^{-2}.$$

In the ferromagnetic state we have

$$\chi_c\approx[\gamma\pm4\beta_2B^{-1/3}(-A_3)^{1/3}]/2(-A_3),$$

and in the limit $A_3\to-0$ we have

$$\chi_c\to\gamma(-2A_3)^{-1}.$$

In the limit $A_3\to-\infty$ we have

$$\chi_c\to\pm2\beta_2B^{-1/3}(-A_3)^{-1/3}.$$

Under the condition $\gamma\beta_2<0$, the function χ_c has some additional features in the ferromagnetic phase: At the point $(-A_3)^{1/2}\approx\mp\gamma B^{1/2}/4\beta_2=\mp A_3^{(0)}/4$, this function takes on a value $\chi_c\approx0$. At the point $(-A_3)^{1/2}\approx\mp A_3^{(0)}/2$, the susceptibility has a local minimum or maximum, $\chi_{c0}\approx-2\beta_2^2/\gamma B$, respectively, under the conditions $\gamma\gtreqless0$. The value $(-A_3)^{1/2}\approx\mp2A_3^{(0)}/3$ corresponds to an inflection point. In the strong-field region, χ_c reaches a minimum or maximum, $\chi_{c0}\approx-4\beta_2^2/3\gamma B$, at the point $H_\Sigma^{1/3}\approx-\gamma B^{1/3}/2\beta_2$ under the conditions $\gamma\gtreqless0$. In the case $H_\Sigma^{1/3}=-\gamma B^{1/3}/4\beta_2$, it takes on the value $\chi_c\approx0$. Near the global maximum we have $\chi_c\propto H_\Sigma^{-2/3}$. It follows from an analysis of the functional dependence $\chi_c(U_0)$ that, for ex-

ample, under the conditions $A, \beta_2, H_\Sigma > 0$, and $\gamma < 0$ an increase in U_0 is accompanied by an increase in χ_c in the paramagnetic phase. It goes through a maximum and then decreases, going negative. In the ferromagnetic state, χ_c increases from the region $\chi_c < 0$, crosses zero, goes through a local maximum, and then asymptotically approaches zero. As the critical point is approached ($A_3, H_\Sigma \to 0$), the maximum of χ_c tends toward infinity, and the power laws have different exponents in the ferromagnetic and paramagnetic states.

In the case $H_\Sigma = 0$, in which the effect of the field H is canceled by the wave, the light will create only uniaxial anisotropy. Assuming $K_{12} = 0$ in the discussion below, and replacing M_z by M_x, we find a phase diagram of the magnetic material in terms of the coordinates H, A.

The self-consistent-field theory is valid only near the phase-transition point, outside the fluctuation region. In this case, the range of applicability is determined by the following conditions, where we are taking the shift of T_C into account:

$$\frac{(BT_{Cc})^2}{A'a^3} \ll \frac{T_C - T_{Cc}}{T_{Cc}} \ll 1,$$

where $T_{Cc} = T_C + \Delta T_C$.

These results become valid for a right-hand circularly polarized wave if we replace α by $-\alpha$ in (10)–(16).

ORIENTATIONAL PHASE TRANSITIONS

At relatively low temperatures ($T \ll T_C$), the magnitude of the magnetization **M** is conserved. In this case, we can conveniently rewrite (4) in polar coordinates:

$$w = {}^1/_2 aM_0^2[(\nabla\theta)^2 + (\nabla\varphi)^2 \sin^2\theta] + {}^1/_4[K_1 \sin^2 2\theta + (K_1 + K_2\cos^2\theta)\sin^4\theta \sin^2 2\varphi] - (U_x \cos^2\varphi + U_y \sin^2\varphi)\sin^2\theta - U_z \cos^2\theta - V_{xy} \sin 2\varphi \sin^2\theta - (V_{xz}\cos\varphi + V_{yz}\sin\varphi)\sin 2\theta - \mathbf{MH}_\Sigma. \quad (17)$$

Here θ and φ are the polar and azimuthal angles of the vector **M**,

$$K_1 = (K_{12} + K_{112}M_0^2)M_0^4, \quad K_2 = (K_{123} - 3K_{112})M_0^6$$

are the crystallographic-anisotropy constants,

$$U_i = (\beta_1 - \beta_2)M_0^2|E_i|^2/16\pi, \quad V_{ij} = \beta_3 M_0^2(E_iE_j^* + E_i^*E_j)/32\pi$$

is the constant of the light-induced anisotropy, M_0 is the saturation magnetization, and

$$E_x = -E_1 \sin\varphi_n - E_2 \cos\theta_n \cos\varphi_n,$$
$$E_y = E_1 \cos\varphi_n - E_2 \cos\theta_n \sin\varphi_n,$$
$$E_z = E_2 \sin\theta_n.$$

Here E_1 and E_2 are field components in the Cartesian coordinate system ($\mathbf{n}, \mathbf{e}_1, \mathbf{e}_2$) moving with the wave, **n** is the unit vector along the wave propagation direction, θ_n and φ_n are the polar coordinates of the vector **n**, and $\mathbf{e}_1$ is a unit vector in the x, y plane. In addition,

$$\mathbf{H}_\Sigma = \mathbf{H} + \mathbf{n}G$$

is the resultant internal magnetic field,

$$G = \alpha|E_1||E_2|\sin\delta/8\pi$$

is the field produced by the light, and $\delta = \delta_1 - \delta_2$ is the phase difference between the components $E_{1,2} = |E_{1,2}| \exp(i\delta_{1,2})$.

We consider uniform phase transitions in the field of a wave which is linearly polarized ($\delta = 0$) along the [001] axis ($E_1 = 0$). The wave is propagating in the basal plane ($\theta_n = \pi/2$) with $H = 0$. In this case, (17) simplifies:

$$w = {}^1/_4[K_1 \sin^2 2\theta + (K_1 + K_2\cos^2\theta)\sin^4\theta \sin^2 2\varphi] - U\cos^2\theta, \quad (18)$$

where $U = U_z$. The effect of the light on the magnetic material reduces in this case to no more than the induction of a uniaxial anisotropy, with an axis parallel to the polarization axis. Working from (18), we can write the equations for stationary states in the form

$$\mu \sin 2\theta = [K_1 \cos 2\theta + {}^1/_2(K_3 - {}^3/_2 K_2 \sin^2\theta) \times \sin^2\theta \sin^2 2\varphi + U] \sin 2\theta = 0,$$
$$\sin 2\varphi \cos 2\varphi (K_1 + K_2\cos^2\theta)\sin^4\theta = 0, \quad (19)$$

where $K_3 = K_1 + K_2$.

The stability of the states is determined by the inequalities

$$\frac{\partial^2 w}{\partial\theta^2} > 0, \quad \frac{\partial^2 w}{\partial\theta^2}\frac{\partial^2 w}{\partial\varphi^2} - \left(\frac{\partial^2 w}{\partial\theta\,\partial\varphi}\right)^2 > 0,$$
$$\partial^2 w/\partial\theta^2 = 2\mu\cos 2\theta - \sin^2 2\theta[2K_1 - {}^1/_2(K_3 - 3K_2\sin^2\theta)\sin^2 2\varphi],$$
$$\partial^2 w/\partial\varphi^2 = 2(K_1 + K_2\cos^2\theta)\sin^4\theta\cos 4\varphi, \quad (20)$$
$$\partial^2 w/\partial\theta\partial\varphi = \sin^2\theta \sin 2\theta (K_3 - {}^3/_2 K_2 \sin^2\theta)\sin 4\varphi.$$

From (19) we find the stationary states; from (18) and (20) we find their energy and the stability region:

1) $\theta^{(1)} = 0, \pi$; $w^{(1)} = -U$; $U \geqslant -K_1$;

2) $\theta^{(2)} = \pi/2$, $\varphi^{(2)} = n\pi/2$, $n = 0, 1, 2, 3$;
$w^{(2)} = 0$; $U \leqslant K_1$, $K_1 \geqslant 0$;

3) $\theta^{(3)} = \frac{\pi}{2}$, $\varphi^{(3)} = \frac{(1+2n)\pi}{4}$; $w^{(3)} = \frac{K_1}{4}$;
$U \leqslant \frac{K_1}{2} + \frac{K_2}{4}$, $K_1 \leqslant 0$;

4) $\theta^{(4)} = \frac{1}{2}\arccos\left(-\frac{U}{K_1}\right)$, $\varphi^{(4)} = \frac{n\pi}{2}$;
$w^{(4)} = \frac{K_1}{4}\left(1 - \frac{U}{K_1}\right)^2$;
$K_1\left(1 + 2\frac{K_1}{K_2}\right) \leqslant U \leqslant -K_1$, $-K_2 \leqslant K_1 \leqslant 0$; (21)

5) $\theta^{(5)} = \arcsin[t + (t^2+s)^{1/2}]^{1/2}$, $\varphi^{(5)} = (1+2n)\pi/4$;
$w^{(5)} = -U + {}^1/_2 K_2[{}^3/_2 ts + t^3 + (t^2+s)^{3/2}]$;
$U \leqslant -K_1$, $K_1 \leqslant -K_2$, $U \leqslant \frac{9}{4}K_2\left(\frac{1}{3} + \frac{K_1}{K_2}\right)$,
$-K_2 \leqslant K_1 \leqslant -\frac{K_2}{3}$, $U \geqslant \frac{1}{2}K_1 + \frac{1}{4}K_2$, $K_1 \leqslant -\frac{3}{2}K_2$,

$$U \geqslant -\frac{3}{4}K_2\left(\frac{1}{3}+\frac{K_1}{K_2}\right), \quad -\frac{2}{3}K_2 \leqslant K_1 \leqslant -\frac{K_2}{3},$$

where $t = 1/3 - K_1/K_2$, and $s = 4/3(U + K_1)/K_2$. The relations for the stability regions with the equal sign determine the line of instability. All the states are degenerate, as can be seen from (21). The reason for this degeneracy is that the axis of the light-induced anisotropy coincides with a symmetry axis of the crystal. In phases 1, 2, and 3, the vector **M** is oriented along the symmetry axes: These are collinear phases. In the state 1, the magnetization vector is directed along the polarization axis. In the states 2 and 3, the vector **M** lies in the plane perpendicular to the polarization axis. The orientation of **M** is along the [100] crystallographic direction in phase 2 and along the [110] direction in phase 3. In the corner phases 4 and 5, the direction of **M** does not coincide with a symmetry axis of the crystal. In state 4, the vector **M** rotates in the (100) plane, while in state 5 it rotates in the (110) plane. In the limit $U \to 0$ we have the asymptotic behavior $\cos 2\theta^{(4)} \to 0$, $\sin^2\theta^{(5)} \to 2/3$. In this case **M** becomes oriented along a face diagonal, [110], or along a body diagonal, [111]; these orientations are the same as in the phases of the cubic magnetic material in the absence of external fields.[11]

The stability of the phases depends on the sign of K_2. If we have $K_2 < 0$, phase 4 is unstable. The stability regions for the different phases may overlap. If we have $K_2 < 0$, then regions 1 and 2, 1 and 3, 3 and 4, 3 and 5, and 4 and 5 overlap. In addition, phases 3, 4, and 5 overlap. If we have $K_2 > 0$, then regions 1 and 2; 1 and 5; 2 and 5; and 1, 2, and 5 overlap. Hysteresis arises upon a transition from one state to another in an overlap region. The stability regions of phases 2 and 3 do not overlap, although the direction of **M** changes abruptly upon a transition between these states.[3)] In a region in which three phases coexist, the energy of one phase is always greater than the two other energies. In the case $K_2 > 0$ with $U > 0$, the inequalities $w^{(3)} > w^{(4)}$, $w^{(5)}$ hold. In the case $U < 0$, the inequalities $w^{(4)} > w^{(3)}$, $w^{(5)}$ hold. If $K_2 < 0$ holds, then $w^{(2)} > w^{(1)}$, $w^{(5)}$ for $U > 0$ or $w^{(1)} > w^{(2)}$, $w^{(5)}$ for $U < 0$.

Equating the energies of coexisting phases, we find the following relations for the phase boundaries:

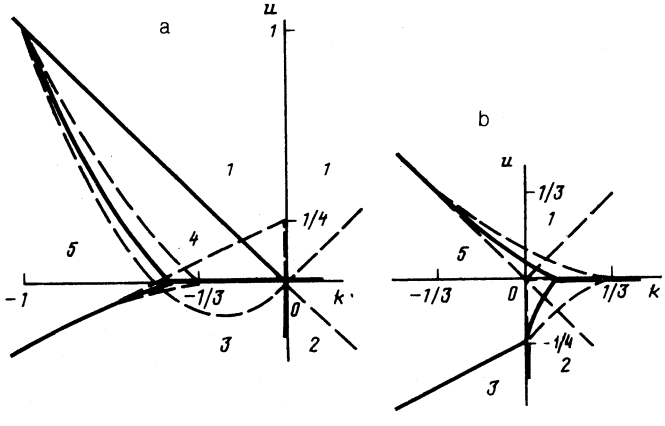

FIG. 2. Phase diagrams of a cubic ferromagnet in the vicinity of a spin-flip phase transition in the field of a linearly polarized wave. a—$K_2 > 0$; b—$K_2 < 0$.

1–2: $u=0$, $k \geqslant 0$, $K_2>0$; $u=0$, $k \geqslant 1/9$, $K_2<0$;
1–4: $u=-k$, $-1 \leqslant k \leqslant 0$, $K_2>0$;
1–5: $u=-k$, $k \leqslant -1$, $K_2>0$; $u=-k$, $k \leqslant -1/3$, $u=-k+9/16(1/3+k)^2$, $-1/9 \leqslant k \leqslant 1/9$, $K_2<0$;
2–3: $u \leqslant 0$, $k=0$, $K_2>0$; $u \leqslant -1/4$, $k=0$, $K_2<0$;
2–5: $u^3+1/2(1-3/2k-9/2k^2)u^2+1/16(1-11k+9k^2+9k^3)u -1/16k^2(1-10k+9k^2)=0$, $0 \leqslant k \leqslant 1/9$, $K_2<0$;
3–4: $u=0$, $-4/9 \leqslant k \leqslant 0$, $K_2>0$;
3–5: $u=1/2(k+1/2 \operatorname{sign} K_2)$, $k \leqslant -2/3$; $u^3-1/2(1+3/2k-9/2k^2)u^2+1/16(1+2k-9/2k^2-9k^3)u +1/64k(1+25/4k+13k^2+9k^3)=0$, $-2/3 \leqslant k \leqslant -4/9$, $K_2>0$; $u=1/2(k-1/2)$, $k \leqslant 0$, $K_2<0$;
4–5: $u=1/27k\{9+2k[10+(3k^{-1}+7)^{1/2}]\}$, $-1 \leqslant k \leqslant -4/9$, $K_2>0$,

(22)

where $u = U/|K_2|$, and $k = K_1/|K_2|$. Figure 2a, b, shows phase diagrams for $K_2 \gtrless 0$, respectively.[12] The heavy lines are boundaries between phases, while the dashed lines are lines of instability which do not coincide with phase boundaries. Transitions between phases when the energy density of the light or the parameters of the magnetic material changes are accompanied by either a continuous change in **M** (PT-II) or an abrupt change in **M** (a first-order phase transition, PT-I). A PT-II transition occurs between phases 1 and 4, 1 and 5, and 3 and 5 in the region $K < -2/3$ in the case $K_2 > 0$. It also occurs between phases 1 and 5 in the region $K < -1/3$ and between phases 3 and 5 in the region $k < 0$ in the case $K_2 < 0$. The transition between phases 2 and 3 is the hysteresis-free transition PT-I. A hysteretic transition PT-I occurs between phases 1 and 2 and between phases 3 and 5 in the region $-2/3 < k < -1/3$ if $K_2 > 0$. It also occurs between phases 1 and 5 in the region $-1/3 < k < 1/3$ and between phases 2 and 5 in the region $0 < k < 1/3$ if $K_2 < 0$.

The critical points have the coordinates $k = -2/3$, $u = -1/12$ for $K_2 > 0$ or $k = -1/3$, $u = 1/3$ for $K_2 < 0$. At these points, the PT-I line with hysteresis gives way to a PT-II line. At the point $k = 0$, $u = 1/4$ for $K_2 > 0$ the line PT-II splits into a line of a hysteresis-free PT-I and a line of a hysteretic PT-I. At the origin of coordinates in the case $K_2 > 0$ the PT-II line splits into two lines, PT-I with hysteresis and PT-I without hysteresis. At the bicritical point, $k = -1$, $u = 1$ for $K_2 > 0$, two PT-II lines and a line of a PT-I with hysteresis converge. At the points $k = -4/g$, $u = 0$ for $K_2 > 0$ or $k = -1/g$, $u = 0$ for $K_2 < 0$, three PT-I lines with hysteresis converge.

The resulting phase diagrams can be used to determine the changes in the components of **M** as a function of the light intensity and the parameters of the material. Figure 3a, b, shows the component $m_z = M_z/M_0$ as a function of the intensity for various relations between β_1 and β_2 ($u \gtrless 0$ for $\beta_1 \gtrless \beta_2$) for $K_2 \gtrless 0$. The dashed lines correspond to points of instability. In the regions $k < -1$ for $\beta_1 > \beta_2$ and $k < -2/3$ for $\beta_1 < \beta_2$ in the case $K_2 > 0$, and in the regions $k < -1/3$ for $\beta_1 > \beta_2$ and $k < 0$ for $\beta_1 < \beta_2$ in the case $K_2 < 0$, the components of **M** vary continuously with increasing **U** in a corner phase and remain constant in the collinear phases. In the interval $-1 < k < -4/g$ in the case $K_2 > 0$ and $\beta_1 > \beta_2$, the vector **M** rotates in the (110) plane with increasing light

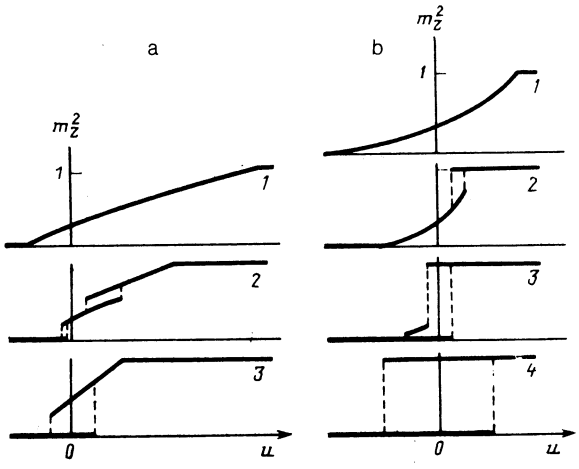

FIG. 3. Square of the component m_z versus the energy density of the wave field. a: $K_2>0$. 1—$k=-1$; 2—-0.55; 3—-0.25. b: $K_2<0$. 1—$k=-0.42$; 2—-0.06; 3—0.06; 4—0.3.

intensity and then turns abruptly to an orientation along the [100] axis (PT-II). In the interval $-2/3<k<-4/9$ for $\beta_1<\beta_2$ in the case $K_2>0$, and in the interval $-1/3<k<1/9$ for $\beta_1>\beta_2$ and also the interval $0<k<1/9$ for $\beta_1>\beta_2$ in the case $K_2<0$, a single transition, PT-I, occurs as the intensity is raised. If the stability regions overlap in the case $u=0$, the change in **M** depends on the original orientation. The components of **M** do not change if the initial orientation of this vector is the same as the asymptotic orientation in the limit $|U|\to\infty$. In the opposite case, a PT-I occurs with increasing U_0. A PT-II may occur later. After the effect of the light ends, the orientation of **M** is not the same as its original orientation: There is hysteresis as U_0 is varied.

In addition to the stable states (20) discussed above, there are some unstable stationary states of the saddle-point type. These states have a significant effect on nonuniformly magnetized magnetic materials.

We now consider reorientation of the vector **M** in the field of a circularly polarized wave which is propagating through a slightly anisotropic magnetic material ($\beta_i M_0^2 U_0, \alpha M_0 U_0 \gg K_1, K_2$) in the direction of the external magnetic field. Working from (11), using the condition $\mathbf{M}^2=M_0^2$, and proceeding as above, we find the stationary states, their energy, and their stability regions:

$$\begin{aligned}
&1)\ \sin\theta^{(1)}=0,\ \cos\varphi^{(1)}=0;\quad w^{(1)}=0;\quad U\gtrless 0 \\
&\qquad\qquad \text{for}\quad \cos\theta^{(1)}\sin\varphi^{(1)}\gtrless 0; \\
&2)\ \sin\theta^{(2)}=1,\ \cos\varphi^{(2)}=1;\quad w^{(2)}=U+F;\quad U\leqslant -F/2; \\
&3)\ \sin\theta^{(3)}=1,\ \cos\varphi^{(3)}=-1;\quad w^{(3)}=U-F;\quad U\leqslant F/2; \\
&4)\ \sin\theta^{(4)}\cos\varphi^{(4)}=-F/2U;\quad w^{(4)}=-F^2/4U;\quad U\geqslant |F|/2,
\end{aligned} \tag{23}$$

where $F=M_0H_\Sigma$. In the metastable state 1, the magnetization is directed normal to the magnetic field. In the collinear phases 2 and 3, **M** is oriented along and opposite the wave propagation direction, respectively. Corresponding to the corner phase 4 are directions of **M** along the generatrix of a cone whose axis is parallel to **H**.

The 2–4 and 3–4 phase boundaries coincide with instability lines. The boundary between phases 2 and 3 is determined by the relations $U\leqslant 0$, $F=0$. The phase diagram is

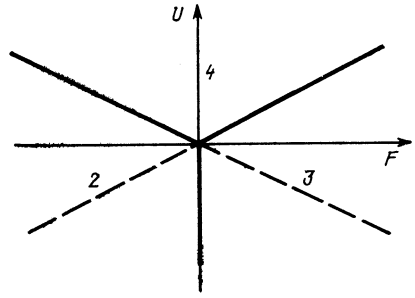

FIG. 4. Phase diagram of a slightly anisotropic ferromagnet in the field of a circularly polarized light wave.

shown in Fig. 4. The transition from phase 4 to phases 2 and 3 occurs through a PT-II. The transition between phases 2 and 3 is a PT-I with hysteresis. We can work from the phase diagram to determine how **M** changes as a result of the light. In the case of an easy-axis light-induced anisotropy ($\beta_1<\beta_2$), under the conditions $H<0$ and $\alpha>0$, the magnetization **M** turns abruptly to an orientation opposite the field as the light intensity is raised. The quantity U_0 reaches a threshold value

$$U_0^{(\text{thr})}=-H/[\alpha+(\beta_1-\beta_2)M_0].$$

For $\alpha<(\beta_2-\beta_1)M_0$, the direction of **M** does not change. In the case of an easy-plane light-induced anisotropy ($\beta_1>\beta_2$), under otherwise the same conditions, the magnetization **M** begins to move away from the H direction for $U_0>U_0^{(\text{thr})}$ and becomes oriented opposite the field at

$$U_0\geqslant -H/[\alpha-(\beta_1-\beta_2)M_0].$$

In contrast with the spontaneous phase transition discussed above, the field does not smear the phase transition in this case; the transition is simply shifted. It thus becomes possible to obtain different types of behavior of the **M** orientation as a function of U_0.

DOMAIN WALLS AND DOMAIN STRUCTURES

The ground state of a ferromagnet of finite dimensions has a domain structure. The size and shape of the domains and also of the walls separating them are determined by the relations among $\mathbf{H}_d$, $\mathbf{H}_0$, the anisotropy field, and the exchange field. Since the light creates an effective magnetic field, an additional anisotropy field, and an additional exchange field, the wave should alter the domain structure and the domain walls.

Varying (17), we find the equations of the inhomogeneous stationary states:

$$aM_0^2\Delta\theta=\partial\bar{w}/\partial\theta,\quad aM_0^2\sin^2\theta\Delta\varphi=\partial\bar{w}/\partial\varphi, \tag{24}$$

where Δ is the Laplacian, and $\bar{w}=w(a=0)$. We consider Bloch domain walls. In this case we find from (24)

$$M_0\int_{\psi_0}^{\psi}(\bar{w}-\bar{w}_0)^{-1/2}\,d\psi=\eta\left(\frac{2}{a}\right)^{1/2}\zeta,$$

$$w_{\text{DW}}=(2a)^{1/2}M_0\int_{\psi_0}^{\psi_1}(\bar{w}-\bar{w}_0)^{1/2}\,d\psi. \tag{25}$$

These expressions give the distribution of **M** in a domain wall and the energy of the wall. In phases 1, 4, and 5 we have $\psi = \theta$, while in phases 2 and 3 we have $\psi = \varphi$. The quantities ψ_0 and ψ_1 are asymptotic values of ψ; $\overline{w}_0 = \overline{w}(\theta_0, \varphi_0)$; ζ is the coordinate normal to the plane of the domain wall; and $\eta = \pm 1$. In the integration of (25) below, we consider only the constant K_1 in cases in which the plane of the domain wall does not coincide with the lateral faces of a cube.

In phase 1, the magnetization distribution in a 180° domain wall is given by

$$\theta_{DW}^{(1)} = \operatorname{arcctg}\left[\left(\frac{U_{1\varphi}}{U+K_1}\right)^{1/2} \operatorname{sh}\left(\frac{\eta\zeta}{\delta^{(1)}}\right)\right], \tag{26}$$

where $\delta^{(1)} = [aM_0^2/2(U+K_1)]^{1/2}$ is a characteristic length, and $U_{1\varphi} = U + \frac{1}{4}K_1 \sin^2 2\varphi$. The angle φ is treated as a parameter in (26); it can take on arbitrary values. Extreme values correspond to angles $n\pi/4$. Far from singular points, the thickness of a domain wall is $\delta_{DW}^{(1)} \approx \pi\delta^{(1)}$ and is determined primarily by the effective anisotropy constant $U + K_1$. With increasing U_0, the quantity $\delta_{DW}^{(1)}$ increases or decreases under the conditions $\beta_1 \lessgtr \beta_2$, respectively. Toward a PT-II line, the thickness of the wall remains finite, $\delta_{DW}^{(1)} \to \pi M_0 (a/2U_{1\varphi})^{1/2}$, and the shape of the wall remains the same. As a PT-I line is approached, a 180° domain wall breaks up into two 90° domain walls between which a new collinear phase forms.

The energy of a domain wall is

$$w_{DW}^{(1)} = w_{DW0}^{(1)} 1+(1+q^{-1})^{-1/2} \begin{cases} q^{-1/2}\operatorname{Arsh} q^{1/2}, & K_1>0, \\ (-q)^{1/2}\arcsin(-q)^{1/2}, & K_1<0, \end{cases} \tag{27}$$

where $w_{DW0}^{(1)} = [2aM_0^2(U+K_1)]^{1/2}$, $q = K_{1\varphi}/U_{1\varphi}$, and $K_{1\varphi} = K_1(1 - \frac{1}{4}\sin^2 2\varphi)$. Domain walls with $\varphi = n\pi/2$ have the minimum energy in the case $K_1 > 0$, while walls with $\varphi = (1+2n)\pi/4$ have the minimum energy in the case $K_1 < 0$. At the point $K_1 = 0$, the plane of the domain wall undergoes reorientation. This rotation of the wall can have strong effects on phase transitions in nonuniformly magnetized magnetic materials.

In phase 2, the magnetization **M** in a wall rotates through an angle of $\pi/2$ in the plane of the base of a cube. The **M** distribution is given by the standard expression

$$\varphi_{DW}^{(2)} = \operatorname{arctg}[\exp(z/\delta^{(2)})], \tag{28}$$

where $\delta^{(2)} = (aM_0^2/K_1)^{1/2}$. In this case the energy is $w_{DW}^{(2)} = (aM_0^2K_1/2)^{1/2}$. The quantities $\delta^{(2)}$ and $w_{DW}^{(2)}$ do not depend on U_0, since **M** always lies in the easy plane. In phase 3, the domain walls are similar to those in phase 2.

In phase 4, the **M** distribution in a domain wall is described by

$$\theta_{DW}^{(4)} = \operatorname{arctg}[\operatorname{tg}\theta^{(4)} \operatorname{th}^{\nu}(x/\delta^{(4)})], \tag{29}$$

where $\delta^{(4)} = (-aM_0^2/2K_1)^{1/2}\cos^{-2}\theta^{(4)}$, $\nu = \pm 1$. The value of ν specifies the interval over which $\theta_{DW}^{(4)}$ varies: $-\nu\theta^{(4)} \leqslant \theta_{DW}^{(4)} \leqslant \nu\theta^{(4)} + (1-\nu)\pi/2$. In a wall with $\nu = 1$, **M** passes through the z axis, while in a wall with $\nu = -1$ it passes through the basal plane. The energy of the wall is given by

$$w_{DW}^{(4)} = w_{DW0}^{(4)} \{\tfrac{1}{2}\sin 2\theta^{(4)} - \cos 2\theta^{(4)}[\theta^{(4)} - (1-\nu)\pi/4]\}, \tag{30}$$

where $w_{DW0}^{(4)} = (-2aM_0^2K_1)^{1/2}$. As the 4–1 phase boundary is approached, we have $\delta_{DW}^{(4)} \to \infty$, $w_{DW}^{(4)} \to 0$ in the case $\nu = 1$ and $\delta_{DW}^{(4)} \to \pi(-aM_0^2/2K_1)^{1/2}$ and $w_{DW}^{(4)} \to (\pi/2)w_{DW0}^{(4)}$ in the case $\nu = -1$. As the 4–2 boundary is approached, the changes in $\delta_{DW}^{(4)}$ and $w_{DW}^{(4)}$ occur in the opposite order. When phase boundaries corresponding to PT-II are crossed, the energy of a wall changes continuously. In phase 5, the domain walls are described by expressions (29) and (30) if K_1 is replaced by $3K_1/4$.

How does the light affect a domain wall? In a plate of a magnetic material with the [111] easy axis ($K_1 < -2K_2/3 < 0$), if this plate is cut in the direction parallel to the (100) plane, there is a stripe domain wall, which is oriented parallel to the [011] axis. A light wave polarized along the [001] axis changes the direction of **M** in the domains and the properties of the domain wall, as we can see from the discussion above. As a result, there are changes in the period (d) and orientation of the domain wall.

The energy of a clearly defined domain wall can be written

$$w = (\overline{w}^{(0)} + 2d^{-1}w_{DW}^{(0)})l + \tfrac{1}{2}\rho M_0^2 d \sin^2\theta_0 \cos^2\varphi_0, \tag{31}$$

where l is the thickness of the plate, $\overline{w}^{(0)} = \overline{w}(\theta_0, \varphi_0)$, $w_{DW}^{(0)} = w_{DW}(\theta_0, \varphi_0)$, θ_0 and φ_0 are the values of the angles in the middle of a domain, and $\rho \approx 1.7$ is numerical coefficient. The terms in (30) determine the energy of the domains, the domain walls, and the demagnetizing fields. The **M** distribution in the domains and in the wall are different from a uniform distribution and different from the distribution of **M** in isolated domain walls, respectively. In the case $d \gg \delta_{DW}$, however, the distinction is negligible. In the case $w_{DW}^{(0)}$ we can thus use the expressions for $w_{DW}^{(i)}$, replacing $\theta^{(i)}$, $\varphi^{(i)}$ by θ_0, φ_0. The energy of a domain wall of the domain structure under consideration is given in this case by

$$w_{DW}^{(0)} = w_{DW0}^{(4)} f, \quad f = \left(\frac{1+3\cos^4\theta_0}{1+\cos^2\theta_0}\right)^{1/2}\left[\frac{1}{2}\sin\theta_0 - \frac{\cos^2\theta_0}{(1+\cos^2\theta_0)^{1/2}}\arcsin\frac{\sin\theta_0}{2^{1/2}}\right]. \tag{32}$$

At $\theta_0 = \pi/2$, the energy in (32) is comparable to $w_{DW}^{(3)}$. Substituting (32) and (18) into (31), and minimizing with respect to θ_0 and d, we find

$$d = d_0 f^{1/2} \sin^{-1}\theta_0, \tag{33}$$

where $d_0 = 2[2l(-2aK_1)^{1/2}/\rho M_0]^{1/2}$. The angle θ_0 satisfies the equation

$$\sin 2\theta_0 \left[\cos^2\theta_0 - \frac{1}{3}\left(1 - 2\frac{U}{K_1}\right) - p\frac{f^{1/2}}{\sin\theta_0}\left(1 + \frac{f'}{2f}\operatorname{tg}\theta_0\right)\right] = 0, \tag{34}$$

where $p = \rho M_0^2 d/(-3K_1 l)$, and $f' \equiv \partial f/\partial\theta_0$. In the domains, as in an unbounded magnetic material, there are two collinear phases, with $\theta_0 = 0$ and $\pi/2$, and there is also a corner phase. Since we have $\cos^2\theta^{(5)} = \frac{1}{3}[1 - 2(U/K_1)]$ if we take only the constant K_1 into account, the value of θ_0 in the corner phase differs only negligibly from $\theta^{(5)}$ if $p \ll 1$. The angle between the polarization axis and the direction of the domain structure is given by

$$\theta_{DS}=\operatorname{arctg}(2^{-1/2}\operatorname{tg}\theta_0). \quad (35)$$

For $\beta_1>\beta_2$, an increase in U_0 is accompanied by decreases in d and θ_{DS}. At small values of θ_0, we find $d\propto\theta_0^{1/2}$ and $\theta_{DS}\sim\theta_0$ from (33) and (35). As the boundary of the nonuniform state is approached, we find d, $\theta_{DS}\to 0$. The reason why d decreases, despite the decrease in the component of **M** normal to the plane, is that the wall energy falls off more rapidly than the energy of the demagnetization fields. Under the condition $\beta_1<\beta_2$, an increase in U_0 is accompanied by increases in d and θ_{DS}. As the vector **M** rotates toward the basal plane we find $d\to d_0(\pi/2)^{1/2}$ and $\theta_{DS}\to\pi/2$. The transition from a nonuniform state with a domain wall making an angle with the crystallographic axes to a uniform state and to a state with a domain wall parallel to the axes occurs through a PT-II.

Near the critical points, this analysis does not hold. It simply indicates the existence of a phase transition but does not describe it. In the limit $\theta\to 0$, the quantity δ_{DW} becomes comparable to d. The difference between a domain wall and domains disappears. The change in the angle θ becomes harmonic. Taking the energy of the demagnetization fields into account, we write w as a series in θ, which we restrict to quadratic terms. From the condition for a minimum of the energy we find the period of the critical mode to be

$$d_c=(4\pi^2 al)^{1/3}. \quad (36)$$

The period d_c is small ($a\sim 10^{-12}$ cm^2) but not zero. Equating the energies of the uniform and modulated states, we find the equation of the phase boundary to be

$$U+K_1+3M_0^2(\pi^2 a/2l^2)^{1/3}=0. \quad (37)$$

The shift of the PT-II line with respect to the uniform phase transitions [see (21)] determined by the last term in (37) increases with increasing inhomogeneous exchange and with decreasing thickness of the plate.

TRANSITIONS TO A NONUNIFORM STATE

A nonuniform state may be caused not only by the demagnetizing fields but also by pinning of the magnetization **M** at defects in the interior or at the surface of the magnetic material. If the magnetic-dipole energy is small in comparison with the energy of the interaction of **M** with the defects, the nonuniformity of the magnetization will be determined primarily by the defects. The effect of the defects strengthens as the phase-transition point is approached.

Let us consider an unbounded plate of thickness l, with a surface which coincides with the lateral faces of a cube. In the absence of an external field, and with K_1, $K_2>0$, the magnetization **M** lies in the plane of the plate and is directed along a [001] or [010] axis. Consequently, demagnetizing fields do not arise. We assume that **M** at the boundaries of the plate is pinned in the [001] direction. In the absence of light, the state will then be uniform (the vector **M** will be parallel to the [001] axis). During the application of a light wave which is polarized linearly along the z axis (the z axis is parallel to the [001] direction), in the case $U<0$, the vector $\mathbf{M}(\mathbf{M}^2=M_0^2)$ rotates in the plane of the plate ($\varphi=\pi/2$). The rotation angle θ reaches a maximum value θ_m at the middle of the plate, while at the surfaces we have $\theta=0$. Substituting (18) into the first equation into (25), and integrating the latter, imposing the boundary conditions, we find an expression which describes the distribution of **M** over the thickness of the plate:

$$\theta=\operatorname{arctg}\left\{\frac{\theta_1(u_1-\theta_2)\operatorname{sn}^2(\eta\xi,\mathfrak{k})}{(u_1+\theta_1)[1-\theta_1\operatorname{sn}^2(\eta\xi,\mathfrak{k})]-\theta_2}\right\}^{1/2}. \quad (38)$$

Here $\theta_1=\sin^2\theta_m$, $\theta_2=\cos^2\theta_m$, $u_1=-U/K_1>\theta_2$, $\operatorname{sn}(\xi,\mathrm{k})$ is the elliptic function, $\xi=[2(u_2+2\theta_1)^{1/2}/ab]x$ is its argument, $u_2=u_1-1$, $a_1=(2aM_0^2/l^2K_1)^{1/2}$, and $\mathfrak{k}^2=\theta_1(u_1+\theta_1)/(u_2+2\theta_1)$ is the modulus of the elliptic function. The quantity θ_m in (38) is found from the equation $(u_2+2\theta_1)^{1/2}=a_1\mathscr{K}$, where $\mathscr{K}(\mathfrak{k}^2)$ is the complete elliptic integral of the first kind.

The energy of the nonuniform state per unit area of the plate can be written as follows, where we are using the second equation in (25):

$$w=lK_1\left[2a_1\int_0^{\theta_m}(\cos^2\theta-\theta_2)^{1/2}(\theta_1+u_2+\sin^2\theta)^{1/2}d\theta+(\theta_1+u_1)\theta_2\right]. \quad (39)$$

Minimizing (39) with respect to θ_m, we find the equation of the stationary states to be

$$\sin 2\theta_m(u_2+2\theta_1)^{1/2}[a_1\mathscr{K}-(u_2+2\theta_1)^{1/2}]=0. \quad (40)$$

Stable stationary states satisfy the condition

$$2(\theta_2-\theta_1)(u_2+2\theta_1)^{1/2}[a_1\mathscr{K}-(u_2+2\theta_1)^{1/2}]+4\theta_1\theta_2\left[a_1\mathscr{K}(u_2+2\theta_1)^{-1/2}+\frac{a_1}{2}\left(\frac{\mathscr{E}}{1-\mathfrak{k}^2}-\mathscr{K}\right)\left(\frac{\partial\ln\mathfrak{k}^2}{\partial\theta_1}\right)(u_2+2\theta_1)^{1/2}-2\right]>0, \quad (41)$$

where $\mathscr{E}(\mathfrak{k}^2)$ is the complete elliptic integral of the second kind. Equation (40) has the solution $\theta_1^{(1)}=0$. The reason for the existence of a uniform solution is that the axis of the surface anisotropy which pins **M** coincides with a crystallographic symmetry axis. It follows from (41) that the uniform state $\theta=\theta_m^{(1)}=0$ is stable in the region $u_2<a_2=\pi^2a_1^2/4$. A solution of Eq. (40) of the form $\theta_2^{(1)}=0$, which describes a nonuniform state with $\theta_m=\pi/2$, is unstable. In the region $\theta_1\ll 1$ we can use the asymptotic ($\mathfrak{k}^2\to 0$) expansion $\mathscr{K}\to\frac{1}{2}\pi(1+\frac{1}{4}\mathfrak{k}^2)$, and we find a solution of (40) in the form

$$\theta_1^{(2)}=-\frac{u_2-a_2}{2}\left[1\mp\left(1-\frac{8u_2(u_2-a_2)}{(8-a_2)(u_2-a_3)^2}\right)^{1/2}\right], \quad (42)$$

where $a_3=5a_2/(8-a_2)$. It follows from (41) that the first solution in (42) is stable for $u_2>3$ in the range

$$u_2>a_2>\max\left\{\frac{8u_2(2+u_2)}{25+u_2(2+u_2)},\ \frac{2u_2(2+u_2)}{5+3u_2}\right\},$$

while the second solution is unstable. The stability regions of phases 1 and 2 have a common boundary $a_2=u_2$. When this boundary is crossed, θ_m changes continuously. In the region $\theta_2\ll 1$, using the asymptotic expansion $\mathscr{K}\to\ln[4/(1-\mathfrak{k}^2)]$ as $\mathfrak{k}^2\to 1$, we can write a solution of (41) in the form

$$\theta_2^{(3)}=16\exp\{-\pi[(2+u_2)/a_2]^{1/2}\}, \quad (43)$$

which is valid for $u_2+2\gg a_2$. The region in which solution (43), with (41), is stable is given by

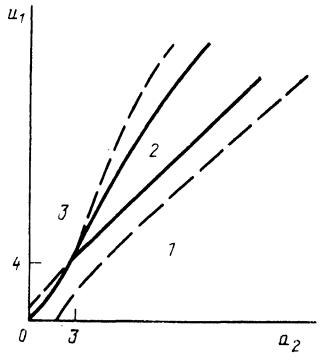

FIG. 5. Phase diagram of a ferromagnetic plate with magnetic moments pinned at the surface in the field of a linearly polarized wave.

$$\pi\left(\frac{2+u_2}{a_2}\right)^{1/2} > \ln\left[\pi\left(\frac{2+u_2}{a_2}\right)^{1/2}\right] + \ln\left[8\left(1+\frac{2}{2+u_2}\right)\right]. \tag{44}$$

This region overlaps the stability regions of phases 1 and 2.

The energy of these states can be expressed in terms of $\mathscr{E}(\mathfrak{k}_i^2)$ and $\mathscr{K}(\mathfrak{k}_i^2)$ on the basis of (39), where $\mathfrak{k}_i^2 = \theta_1^{(i)}$, $i = 2, 3$. The integrals $\mathscr{E}$ and $\mathscr{K}$ can be written as series in $\mathfrak{k}_2^2$, and $1 - \mathfrak{k}_3^2$ in which only the first terms are retained. In this case, the phase boundaries are given by

$$\begin{aligned}
&1-2: \quad && u_1 = a_2 + 1,\\
&2-3: \quad && u_1(\theta_2^{(2)} - \theta_2^{(3)}) = a_1 u_2^{1/2}[2 - {}^1/_2\pi\theta_1^{(2)}\\
& && \quad -({}^1/_2 + 2\ln 2 - {}^1/_2 \ln\theta_2^{(3)})\theta_2^{(3)}],\\
&1-3: \quad && u_1 = 2a_1(\theta_1^{(3)} + u_2)^{1/2}[1 - (\ln 2 - {}^1/_4 \ln\theta_2^{(3)} + {}^1/_4)\theta_2^{(3)}]\\
& && \quad + (u_1 + \theta_1^{(3)})\theta_2^{(3)} \quad \text{for} \quad u_1 \ll 1,\\
& && (u_1 - \theta_2^{(3)})\theta_1^{(3)} = a_1\{(\theta_1^{(3)})^{1/2}(\theta_1^{(3)} + u') + u'\ln([\theta_1^{(3)}\\
& && + (\theta_1^{(3)} + u')^{1/2}](u')^{-1/2})\} \quad \text{for} \quad u_1 \gg 1,
\end{aligned} \tag{45}$$

where $u' = u_1 - \theta_2^{(3)}$. The phase diagram is shown in Fig. 5. The transition between phases 1 and 2 is of second order, while that between phases 1 and 3 and that between phases 2 and 3 are of first order. With increasing intensity of the light, at a fixed $a_2 > 3$, the value of θ_m is zero as long as the condition $u_2 < a_2$ holds. Later on, θ_m begins to increase monotonically, but remains small. When the instability boundary of phase 2 is reached, the value of θ_m changes abruptly to a high value. After this jump, θ_m monotonically approaches $\pi/2$. With increasing intensity, θ_m jumps into phase 1 abruptly, skipping phase 2.

The boundary condition used above holds as long as the surface-anisotropy field is weaker than the nonuniform-exchange field. In the opposite case, the magnetization **M** undergoes a reorientation of the surface, so the distribution of **M** in the interior changes. When the phase transition at the surface is taken into account, the phase diagram of the magnetic material becomes more complicated.

We thus see that defects can substantially alter the reorientation of **M**. Certain previously stable uniform states may become unstable, and the stability region of other uniform states may expand. Some new stable states, both nonuniform and uniform, arise.

DISCUSSION OF RESULTS

We have been discussing cubic magnetic materials. In general, one can introduce an effective field due to the light wave as follows:

$$\tilde{\mathbf{H}}_E = -\delta w_E/\delta\mathbf{M}, \tag{46}$$

where $w_E = w(E_i, \partial E_i/\partial x_j)$. If w depends on E_i alone, the expression for $\tilde{\mathbf{H}}_E$ can be written

$$\tilde{H}_{Ei} = (ie_{ijk}\alpha_{kn} + 2\beta_{ijkn}M_k + \beta'_{ijkn}H_k)E_j^* E_n/16\pi. \tag{47}$$

The first term in (47) is an analog of the vector product in expression (4). Substituting the effective field in the form $\tilde{\mathbf{H}} = \tilde{\mathbf{H}}_M + \tilde{\mathbf{H}}_E$, where $\tilde{\mathbf{H}}_M$ is the field in the absence of the light, into the equation of motion for **M**, and using (3), we can determine the dynamic and static properties of any magnetic materials.

The calculations above ignored the absorption of the light and the inverse effect of the magnetic subsystem on the light wave. These simplifications are justified if the decrease in the amplitude and the change in the phase of the wave due to the magnetization **M** over the length l of the sample are small. This condition places a limit on the size of the material along the light propagation direction: $l \ll \min(\lambda/2\pi\Delta n, \alpha_{ab}^{-1})$, where λ is the wavelength, Δn is the change in the refractive index due to the magnetization, and α_{ab} is the absorption coefficient. The reorientation of **M** caused by the light may occur even if the condition on l does not hold. There may be changes in not only the phase diagram but also the kinetics of the transition.

The strength of the field $\tilde{\mathbf{H}}_E$, which has a significant effect on the magnetic subsystem, depends on how closely the point of the phase transition can be approached. In the case of magnetic orientational phase transitions, the fluctuation region is very narrow,[13] $\Delta T/T_C \leqslant 10^{-6}$. The proximity to the phase transition is thus determined by the experimental conditions and the quality of the samples. The field $\tilde{\mathbf{H}}_E$ can be estimated from $\tilde{H}_E \approx 2\Delta n I/cM_0$, where I is the light intensity. If the effective internal field is stabilized within ΔH, the relation $\tilde{H}_E > \Delta H$. should hold.

The highest values of Δn are observed in magnetic semiconductors. In EuS ($T_C \approx 16$ K), at $T \approx 8$ K and $\lambda \approx 0.6\,\mu$m, we have $\Delta n_K \approx 0.3$ for the case of circular birefringence, with $\alpha_{ab} \approx 10^5$ cm^{-1} and $M_0 \approx 1.6\times 10^3$ G (Refs. 14–17). In EuO films ($T_C \approx 70$ K) at $T \approx 20$ K, and $\lambda \approx 0.6\,\mu$m, the quantity Δn_K is about 0.25, and we have $\alpha_{ab} \approx 10^5$ cm^{-1} and $M_0 \approx 1.9\cdot 10^3$ G (Refs. 14 and 18). Single crystals of EuSe ($T_C \approx 4.6$ K) are distinguished by their relatively low absorption, $\alpha_{ab} \approx 45$ cm^{-1}, while $\Delta n_K \approx 6.10^{-2}$ is large in the region $\lambda \approx 0.76\,\mu$m at $T \approx 4.2$ K and $M_0 \approx 1.5\cdot 10^3$ G (Refs. 14 and 19). The linear birefringence in EuSe is determined by the value[19] $\Delta n_L \approx 10^{-2}$. The value of Δn is slightly lower in the slightly anisotropic spinels $CdCr_2Se_4$ ($T_C \approx 106$ K). At $T \approx 11$ K and $\lambda \approx 1\,\mu$m we have $\alpha_{ab} \approx 10^3$ cm^{-1} and $M_0 \approx 300$ G, and the value of Δn_K is $\approx 2\cdot 10^{-2}$ (Ref. 20).

Iron garnets have Δn values smaller than those of magnetic semiconductors. However, the high technological level of the synthesis of these materials makes it possible to produce high-quality samples with a wide range of parameter values.[21] These samples are thus preferable experimentally. In iron garnets containing bismuth, at $T \approx 300$ K and at a

wavelength of 0.63 μm, we have $\Delta n_K \approx 10^{-2}$ and $\alpha_{ab} \approx 10^3$ cm^{-1} (Refs. 21 and 22). The absorption coefficient can be lowered to 58 cm^{-1} by adding small amounts of calcium,[23] in which case we obtain $\Delta n_L \approx \Delta n_K$. The constants of the induced anisotropy and the growth anisotropy can be reduced to essentially zero by choosing the appropriate film growth conditions and the appropriate film composition.[21] The value of M can also be varied over a wide range.[22] Using the values given above, we find a field $\tilde{H}_E \approx 0.1$ Oe, roughly the same for all materials, at $I \approx 10^6$ W/cm^2. Experimentally, it is completely feasible to stabilize the internal field at this accuracy level and thus to approach the phase transition in terms of $\tilde{H}_E$.

The shift of T_C can be estimated from $\Delta T_C \approx 4\Delta n I / cA' M_0^2$. Using the parameter values given above for iron garnets containing bismuth, and assuming $A' \approx 10 K^{-1}$ and $M_0 \approx 30$, we find $\Delta T_C \approx 10^{-2}$ K at $I \approx 10^7$ W/cm^2. The magnitude of this shift is comparable to the fluctuation region.

Let us estimate the period and orientation of the domain structure. Assuming that **M** is deflected from a body diagonal through a small angle by the light, we can write the relative change in the period as follows, where we are using (33):

$$\frac{\Delta d}{d_1} = \frac{(5\theta_1 - 2^{1/2})U}{2(2^{1/2} - \theta_1)} \approx \frac{6\Delta n I}{cK_1},$$

where $\theta_1 = \arccos(3^{-1/2})$ is the polar angle of the [111] axis, and d_1 is the period of the domain structure which corresponds to the angle θ_1. Substituting the parameter values used above for the iron garnets into this expression, and assuming that we have $K_1 \approx 6 \cdot 10^2$ erg/cm^3 near the phase transition, we find $\Delta d / d_1 \approx 0.01$ at $I \approx 10^6$ W/cm^2. The rotation of the domain structure caused by the light when the vector **M** deviates very slightly from the [111] axis can be estimated from

$$\Delta\theta_{DS} \approx 3\Delta n I / 2cK_1.$$

Using the same numerical values as in the estimate of Δd, we find $\Delta\theta_{DS} \approx 3.10^{-3}$. At small values of θ_0, we find the ratio $\Delta d / d \approx \Delta\theta_0 / \theta_0$. With decreasing θ_0, the relative change in the period of the domain structure increases.

We should point out that a magnetic material can be brought toward a phase transition not only by varying the anisotropy constants through a change in temperature but also by applying external fields. For example, a stress along the z axis creates an additional uniaxial anisotropy, which shifts the phase diagrams in Fig. 2 along the ordinate, downward or upward, depending on the sign of the magnetostriction constant. A light beam can be applied locally to a magnetic material. This capability adds to the experimental possibilities.

I wish to thank V. G. Veselago, A. K. Zvezdin, and F. V. Lisovskiĭ for a discussion of this study.

[1)] The interaction of the magnetic component of the field can be ignored since the magnetic susceptibility is nearly zero at optical frequencies.
[2)] The point $H_\Sigma = 0$ corresponds to a first-order spin-flip phase transition.
[3)] A correct description of a first-order phase transition between states 2 and 3 would require consideration of the higher-order anisotropy constants. Such corrections require tedious calculations, in which the physics of the effects would be obscured. We accordingly treat the transition between phases 2 and 3 as hysteresis-free, with the understanding that when the additional constants are taken into account the line of this transition will split, either on the line of a second-order phase transition with a corner phase between them, or on the line of loss of stability bounding the hysteresis region.

[1] L. P. Pitaevskiĭ, Zh. Eksp. Teor. Fiz. **29**, 1450 (1960).
[2] P. S. Pershan, I. P. van der Ziel, and L. D. Malmstrom, Phys. Rev. **143**, 574 (1966).
[3] G. M. Genkin and I. D. Tokman, Fiz. Tverd. Tela (Leningrad) **25**, 276 (1983) [Sov. Phys. Solid State **25**, 155 (1983)].
[4] B. A. Zon and V. Ya. Kupershmidt, Zh. Eksp. Teor. Fiz. **84**, 629 (1983) [Sov. Phys. JETP **57**, 363 (1983)].
[5] G. M. Genkin and I. D. Tokman, Fiz. Tverd. Tela (Leningrad) **22**, 1271 (1980) [Sov. Phys. Solid State **22**, 742 (1980)].
[6] B. A. Zon and V. Ya. Kupershmidt, Fiz. Tverd. Tela (Leningrad) **25**, 1231 (1983) [Sov. Phys. Solid State **25**, 708 (1983)].
[7] A. M. Balbashov, B. A. Zon, V. Ya. Kupershmidt *et al.*, Zh. Eksp. Teor. Fiz. **94**(5), 304 (1988) [Sov. Phys. JETP **67**, 1039 (1988)].
[8] V. F. Kovalenko and E. L. Nagaev, Usp. Fiz. Nauk **148**, 561 (1986) [Sov. Phys. Usp. **29**, 297 (1986)].
[9] U. V. Valiev, A. K. Zvezdin, G. S. Krinchik *et al.*, Zh. Eksp. Teor. Fiz. **85**, 311 (1983) [Sov. Phys. JETP **58**, 181 (1983)].
[10] B. A. Zon, V. Ya. Kupershmidt, G. V. Pakhomov, and T. T. Urazbaev, Fiz. Tverd. Tela (Leningrad) **31**(4), 294 (1989) [Sov. Phys. Solid State **31**(4), 717 (1989)].
[11] K. P. Belov, A. K. Zvezdin, R. Z. Levitin *et al.*, Zh. Eksp. Teor. Fiz. **68**, 1189 (1975) [Sov. Phys. JETP **41**, 590 (1975)].
[12] A. F. Kabychenkov, in *Abstracts, XII All-Union School and Seminar on New Magnetic Materials for Microelectronics*, Mashinform, Novgorod, 1990, Chap. 2, p. 44.
[13] K. P. Belov, A. K. Zvezdin, A. M. Kadomtseva, and R. Z. Levitin, *Orientational Phase Transitions in Rare Earth Magnetic Materials*, Nauka, Moscow, 1979, p. 35.
[14] R. V. Pisarev, in *Physics of Magnetic Dielectrics* (ed. G. A. Smolenskiĭ), Nauka, Leningrad, 1974, p. 419.
[15] P. Wachter, CRC Crit. Rev. in Sol. State and Mater Sci. **3**, 189 (1972).
[16] I. Schoenes and P. Wachter, Solid State Commun. **15**, 1891 (1974).
[17] K. Tu, K. Ahn, and I. Suits, IEEE Trans. Magn. **MAG-8**, 651 (1972).
[18] K. Y. Ahn and M. W. Shafer, J. Appl. Phys. **41**, 1260 (1970).
[19] J. C. Suits, B. E. Argyle, and M. J. Freiser, Appl. Phys. **37**, 1391 (1966).
[20] L. L. Golik and Z. E. Kun'kova, Fiz. Tverd. Tela (Leningrad) **22**, 877 (1980) [Sov. Phys. Solid State **22**, 512 (1980)].
[21] P. Hansen and J.-P. Krumme, Thin Solid Films **114**, 69 (1984).
[22] P. Hansen, K. Witter, and W. Tolksdorf, Phys. Rev. B **27**, 4375 (1983); J. Appl. Phys. **55**, 1052 (1984); IEEE Trans. Magn. **MAG-20**, 1099 (1984).
[23] M. Kaneko, T. Okamoto, H. Tamada *et al.*, Appl. Phys. A **38**, 281 (1985).

Translated by D. Parsons